International Journal of Environmental Sciences
ISSN: 2229-7359
Vol. 11 No. 18s, 2025
https://theaspd.com/index.php

Formulation And Characterization Of Novel Formulation Of Terpineol

Ms. Pradnya K. Pehere[1], Dr. Dharmendra Ahuja[2]
[1]Research Scholar of Faculty of Pharmaceutical Sciences, Pradnyapehere93@gmail.com
[2]Dean, Faculty of Pharmaceutical Sciences, Jayoti Vidyapeet Women's University, Jaipur, Rajasthan, India-303122

Abstract
The encapsulation of essential oils into nanocarriers offers a promising strategy to enhance their stability, bioavailability, and controlled release properties for pharmaceutical, cosmetic, and food applications. This study focuses on the formulation and evaluation of essential oil nanocapsules using a suitable polymeric or lipid-based encapsulation system. Essential oils were selected for their known therapeutic properties, and nanocapsules were prepared using techniques such as nanoprecipitation or emulsification–solvent evaporation. The formulated nanocapsules were characterized in terms of particle size, zeta potential, encapsulation efficiency, morphology, and in vitro release profile. Stability studies and bioactivity assessments, including antimicrobial and antioxidant assays, were also conducted. scanning electron microscopy (SEM) and transmission electron microscopy (TEM) for morphological assessment, and Fourier-transform infrared spectroscopy (FTIR) to investigate chemical interactions. Encapsulation efficiency and drug loading capacity were determined through UV-Vis spectroscopy or HPLC, while in vitro release studies were conducted using dialysis methods. Additionally, thermal stability was assessed via differential scanning calorimetry (DSC), and bioactivity assays including antioxidant and antimicrobial tests were performed to evaluate functional efficacy. The results demonstrate that nanocapsulation significantly enhances the physicochemical stability and biological efficacy of essential oils, suggesting their potential in targeted delivery and extended shelf life in various applications. They are employed in areas such as genetic engineering, cosmetics, household cleaning products, and wastewater treatment. Furthermore, they play a crucial role in the delivery of adhesive agents, and have promising uses in cancer therapy and neuroprotective treatments due to their targeted delivery and controlled release capabilities.
Keywords *- Nanocapsules,terpineol, Neuroprotectants, DSC, FTIR, Release kinetics etc*

INTRODUCTION

Nanotechnology has opened new frontiers in drug delivery, particularly in targeting complex disorders of the central nervous system (CNS). Among the various nanocarrier systems developed, **nanocapsules** have emerged as a highly promising platform due to their core–shell structure, which allows the encapsulation of bioactive compounds while enabling **controlled release**, **enhanced stability**, and **targeted delivery**. Nanocapsules typically consist of an oily or aqueous core enclosed within a biodegradable polymeric or lipid-based shell, making them suitable for encapsulating both hydrophilic and lipophilic substances.In recent years, there has been increasing interest in the development of **neuroprotective therapies** aimed at preventing or slowing the progression of neurodegenerative disorders such as **Alzheimer's disease**, **Parkinson's disease**, and **stroke-induced neuronal damage**. Many plant-derived **essential oils** possess potent **antioxidant**, **anti-inflammatory**, and **neuroprotective** properties, but their clinical use is limited by poor solubility, high volatility, and instability under physiological conditions. Encapsulation of these essential oils into nanocapsules offers a viable strategy to **enhance their bioavailability**, **protect them from degradation**, and **facilitate their transport across the blood–brain barrier**.Nanocapsules with high reproducibility and stability are being explored not only in neurotherapeutics but also across diverse life science applications, including **genetic engineering**, **cosmetic delivery**, **cleaning formulations**, and **wastewater treatment**. However, their role in **neuroprotection** is of particular interest due to the complexity of CNS delivery and the need for targeted therapeutic action with minimal systemic side effects.

Essential oils are unstable and fragile volatile compounds. Therefore, they could be degraded easily (by light, temperature, oxidation, volatilization) if they are not protected from external factors. These

protections could increase their action duration and provide a controlled release. Essential oils stability can be increased by encapsulation .

- Nano encapsulation Technique
- Chemical Methods
- Physicochemical Methods
- Mechanical Methods
- Emulsifiers/wall materials used for essential oils
- Encapsulation in liposomes

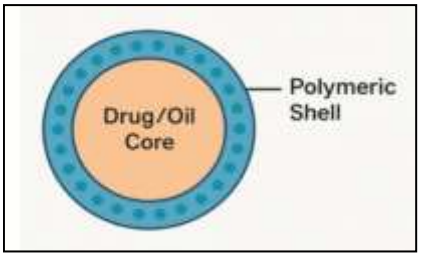

Preformulation characterization

i) Basic Characterization of Terpineol

a. Organoleptic Properties

The organoleptic characteristics of Terpineol were evaluat ion under standard laboratory conditions:

- **Appearance:** The physical form and consistency of the sample were observed visually in ambient light conditions.
- **Odour:** The characteristic aroma of Terpineol was assessed by gently wafting the sample's vapors toward the nose to avoid olfactory fatigue.
- **Taste:** A cautious sensory evaluation was performed by a trained panel using a minimal quantity of the compound, following proper ethical and safety protocols.
- **Color:** The color of the sample was recorded against a white background to ensure accuracy and eliminate background interference.

b. Solubility Profile

The solubility of Terpineol was assessed qualitatively by introducing a small, measured amount of the compound into separate test tubes containing different solvents, including methanol, ethanol, isopropyl alcohol (IPA), acetonitrile, and distilled water. The extent of solubility was observed visually, and the degree of dissolution was noted for each solvent to determine its polarity-based solubility behavior.

c. Physical constant

The boiling point & melting point of Terpineol was determined using the capillary tube method. .

ii. Identification by using UV Spectrophotometer

Standard Terpineol was used to make a series of dilution and a calibration curve was constructed. For diluent purpose, a mixture of acetone and water (50:50) was used, as the nanocapsule preparation had a mixture of these solvent system. Lambda max was previously noted at 249 nm. So for current studies, wavelength was taken as 240 nm.

iii.ATR–FTIR

Infrared (IR) spectral analysis of Terpineol was carried out using the Attenuated Total Reflectance–Fourier Transform Infrared Spectroscopy (ATR–FTIR) technique to identify characteristic functional groups and confirm its chemical structure. A Bruker Platinum ATR spectrometer was used for the analysis. Since Terpineol is a liquid at room temperature, a small amount (1–2 drops) was placed directly onto the clean ATR crystal without any prior sample preparation. A background spectrum was first recorded using a clean and dry crystal to account for atmospheric interference. The sample was then applied, and gentle pressure was applied using the pressure arm to ensure adequate contact with the crystal surface. Spectra were recorded in the range of 4000–400 cm^{-1} at a resolution of 4 cm^{-1}, averaging 32 scans to improve signal quality. After spectral acquisition, the ATR crystal was cleaned thoroughly with ethanol and dried. The obtained IR spectrum was analyzed for characteristic functional group vibrations to confirm the identity and purity of Terpineol.

iv. NMR of Terpineol

The proton nuclear magnetic resonance (^1H NMR) spectrum of Terpineol was recorded using a Bruker 400 MHz NMR spectrometer to confirm its structural identity. Approximately 10 mg of Terpineol was accurately weighed and dissolved in 0.7 mL of deuterated chloroform ($CDCl_3$), and the solution was transferred into a clean, dry 5 mm NMR tube. The analysis was conducted at room temperature using tetramethylsilane (TMS) as the internal standard, with the reference chemical shift set at δ = 0.00 ppm.

The spectral acquisition parameters included 16 scans (NS), a spectral width of 8223.685 Hz, and a relaxation delay (D1) of 1.0 second. The FID was Fourier transformed, and the resulting spectrum was phase and baseline corrected. Chemical shifts were referenced to the residual solvent peak of $CDCl_3$ at δ = 7.26 ppm. The processed spectrum was then analyzed to identify characteristic proton signals corresponding to the molecular structure of Terpineol.

v. DSC of Terpineol

The thermal behavior of Terpineol was investigated using differential scanning calorimetry (DSC) with a Mettler-Toledo DSC system (Switzerland). Approximately 1 mg of the sample was accurately weighed and sealed in a standard aluminum pan. The sample was initially equilibrated at 25°C for 10 minutes before being subjected to a controlled heating program. The analysis was carried out from 25°C to 300°C at a constant heating rate of 10°C per minute under a nitrogen purge at a flow rate of 20 mL/min to maintain an inert atmosphere. The resulting DSC thermograms, recorded as a plot of heat flow (mW) versus temperature (°C), were analyzed to identify characteristic thermal transitions, such as melting point and phase changes, associated with the physicochemical properties of Terpineol.

vi.. Purity Study by gas Chromatography

Analysis of Terpineol by GC-FID:

Table 1: Chromatographic conditions

Sr. No.	Parameter	Set Condition
1	Injection Volume	0.5 µl
2	Injector Temp.	300°C
3	Split Ratio	1:50
4	Carrier Gas	Nitrogen
5	Column	HP-5 (30m x 0.32mm x 0.25 µm)
6	Flow rate	1 ml/min
7	Oven Program	Initial 50°C to 190°C at 10°C/min, then 190°C to 300°C at 10°C/min
8	Runtime	25 minutes
9	FID temperature	300°C
10	Diluent	Tetrahydrofuran

vii. Drug-Excipient compatibility study

Physical mixtures of Oil with polymers like Eudragit L 100, Chitosan, Polysorbate 60 etc was prepared by mixing in 1:1 ratio. To check the compatibility of Terpineol with all excipients and vehicles, their respective mixture were at 50°C for 4 weeks and observed for Terpineol content (%Assay) by UV Spectrophotometer.

MATERIALS AND METHODS

All research chemicals were purchased from from New Neeta Chemicals, PCMC, Pune. All chemicals used were of analytical grade and used as received.

Terpineol , chitosan ,1% v/v aqueous acetic acid solution ,CAA solution , 2M NaOH solution. Tween 80 . Sodium Tripolyphosphate solution (TPP), deionized water are mainly used.

2. Methods:

Terpineol and chitosan was added to 1% v/v aqueous acetic acid solution with continuous mixing/ stirring in a water bath at 60°C for 2 h. The pH value of the CAA solution was adjusted to 4.8 using a 2M NaOH solution. Tween 80 was added to the solution. The homogenous emulsion was obtained through magnetic stirring at 60 °C for 1 hr.

It was stirred under magnetic force for another hour to form a Terpineol and chitosan oil-in-water emulsion at room temperature. Subsequently, Sodium Tripolyphosphate solution (STPP) was included in the emulsion. It underwent 2 hrs. of stirring to crosslink. The sediment was collected via washing at

8000 rpm for 15 min, followed by dispersion in deionized water. The precipitate was collected and vaccum dried and stored in refrigerator at 4^0C until for testing.

Optimization of Terpineol Nanocapsules by using Design Expert

1. Design Expert:

File Version	13.0.5.0		
Study Type	Response Surface	**Subtype**	Randomized
Design Type	Central Composite	**Runs**	9.00
Design Model	Quadratic	**Blocks**	No Blocks

Factors

Factor	Name	Units	Type	SubType	Minimum	Maximum	Coded Low	Coded High	Mean	Std. Dev.
A	Chitosan Conc	mg	Numeric	Continuous	300.00	500.00	-1 ↔ 300.00	+1 ↔ 500.00	400.00	86.60
B	STPP Conc	mg	Numeric	Continuous	50.00	150.00	-1 ↔ 50.00	+1 ↔ 150.00	100.00	43.30

Responses

Response	Name	Units	Observations	Minimum	Maximum	Mean	Std. Dev.	Ratio
R1	Particle Size	nm	9.00	93.4	309.3	188.20	90.21	3.31
R2	Entrapment Efficiency	%	9.00	66.05	77.56	71.52	4.33	1.17

3.Evaluation of Terpineol Nanocapsules

The prepared Terpineol-loaded nanocapsules were evaluated based on various physicochemical, morphological, and structural parameters as described below:

3.1 Physical Appearance

The physical appearance of the nanocapsules was evaluated visually for color, texture, and the presence of any aggregates. Observations were recorded immediately after preparation and during storage to assess stability.

3.2 pH Measurement

The pH of the nanocapsule dispersion was measured using a calibrated digital pH meter (Thermo Orionstar A211). The sample was gently stirred before measurement to ensure uniformity, and pH was recorded at room temperature.

3.3 Active Content Determination

The active content of Terpineol in the nanocapsules was quantified using UV-Visible spectrophotometry. A known volume of nanocapsule dispersion was diluted appropriately with a diluent (methanol) and the absorbance was measured at 240 nm against a blank. The Terpineol concentration was calculated using a previously constructed calibration curve.

3.4 Particle Size Analysis

The particle size was determined by Horiba SZ-100 (Horiba Scientific) at 25℃ using disposable sizing cuvette keeping the refractive index viscosity and dielectric constant as constant.The mean particle size and polydispersity index (PDI) of the nanocapsules were determined using a dynamic light scattering

(DLS) technique. Samples were diluted suitably with deionized water to avoid multiple scattering effects before measurement.

3.5 Zeta Potential Measurement

The surface charge (zeta potential) of the nanocapsules was measured using a zeta potential analyzer i.e. Horiba SZ-100 (Horiba Scientific) at 25°C. Proper dilution with conductivity- Vadjusted water was carried out to ensure accurate measurements. Zeta potential values were used to predict the colloidal stability of the formulation.

3.6 Differential Scanning Calorimetry (DSC)

DSC analysis was carried out to study the thermal behavior of the nanocapsules. Samples were weighed and placed in aluminum pans and scanned over a temperature range (typically 30°C to 300°C) under a nitrogen atmosphere at a heating rate of 10°C/min. Thermograms were analyzed to assess the physical state and any possible interactions between Terpineol and the polymer/excipients used.

3.7 Scanning Electron Microscopy (SEM)

The surface morphology and structural characteristics of the nanocapsules were examined using SEM. A drop of the sample was placed on a metallic stub, dried under vacuum, and coated with a thin layer of gold before imaging. SEM provided high-resolution images of the nanocapsule shape and surface texture.

3.8 Encapsulation Efficiency

Encapsulation efficiency (EE) was determined by separating the unencapsulated free methyl eugenol from the nanocapsule dispersion through ultracentrifugation at 15,000 rpm for 30 minutes. The amount of free drug in the supernatant was quantified spectrophotometrically at 249 nm. Encapsulation efficiency was calculated using the formula:

$$\%\ Entrapment\ efficiency = \frac{Total\ Oil\ Content - free\ oil\ content}{Total\ Oil\ content} \times 100$$

3.9 In-vitro studies using Dialysis Bag study

A dialysis approach was employed to conduct an in vitro release investigation. The dialysis bag was immersed in distilled water to eliminate preservatives and subsequently rinsed with phosphate-buffered saline (PBS) solution. The nanocapsules containing essential oil were redispersed in 3 mL of PBS solution and placed in a dialysis bag, which was surrounded by 50 mL of PBS with 20% ethanol at pH 7.4. A time-dependent release research was conducted over a duration of 0 to 12 hours. All sets were incubated at 37°C with mild agitation. At specific time intervals, 3 mL of the medium was extracted and substituted with new medium, followed by spectrophotometric quantification.

3.10 Release kinetics

The mechanism of drug release and release rate kinetics from the floating microspheres were studied by subjecting in vitro drug release studies into various kinetics models, Zero order, First order, Higuchi matrix and Korsmeyer Peppas model. Zero order as cumulative amount of drug released Vs time, First order as log cumulative percentage of drug remaining Vs time, and Higuchi's model as cumulative percentage of drug released Vs square root of time. The best fit model was confirmed by the value of correlation coefficient near to 1.

3.11 Stability study of TP Nanocapsules

The stability studies were conducted according to ICH guidelines. The stability of TP Nanocapsules was determined by keeping the optimized formulation (F7) at 40°C ± 2°C and 75% ± 5% relative humidity. The samples were tested on 0th day and 90th day for % Drug content, Particle size, zeta potential and SEM.

4 RESULT & DISCUSSION

4.1 Physicochemical Characterization of Terpineol

i) Basic Characterization of Terpineol

The Terpineol was evaluated for various characteristics and the results are given in below:

a) Organoleptic Properties

The Terpineol was evaluated for appearance, taste, colour and odour, and the results are given in Table 7.25.

Table 2: Results Organoleptic Properties of Terpineol

Parameter	Terpineol
Appearance	Terpineol is a Colourless, viscous liquid with a floral odor.
Colour	colorless
Taste	mildly bitter taste
Odour	pleasant, lilac-like floral aroma
Boiling Point	217°C
Flash Point	93°C
Density	0.935 g/cm^3

4.2. Solubility

Terpineol is sparingly soluble in water (approx. 0.1–0.2 g/100 mL) but freely soluble in alcohol, ether, and other organic solvents, making it suitable for formulations requiring lipid solubility.

4.3. Physical constant

The melting point of Terpineol was determined to be approximately -35 °C.

4.4. Identification by using UV Spectrophotometer

A UV-Visible spectrophotometric scan of Terpineol was performed to identify its maximum absorbance wavelength (λmax). The scan showed λmax at 240 nm, which was selected for all subsequent absorbance measurements. Methanol was used as the diluent due to its low UV cut-off at 210 nm, thereby minimizing background interference at the selected wavelength and ensuring accurate spectrophotometric analysis.

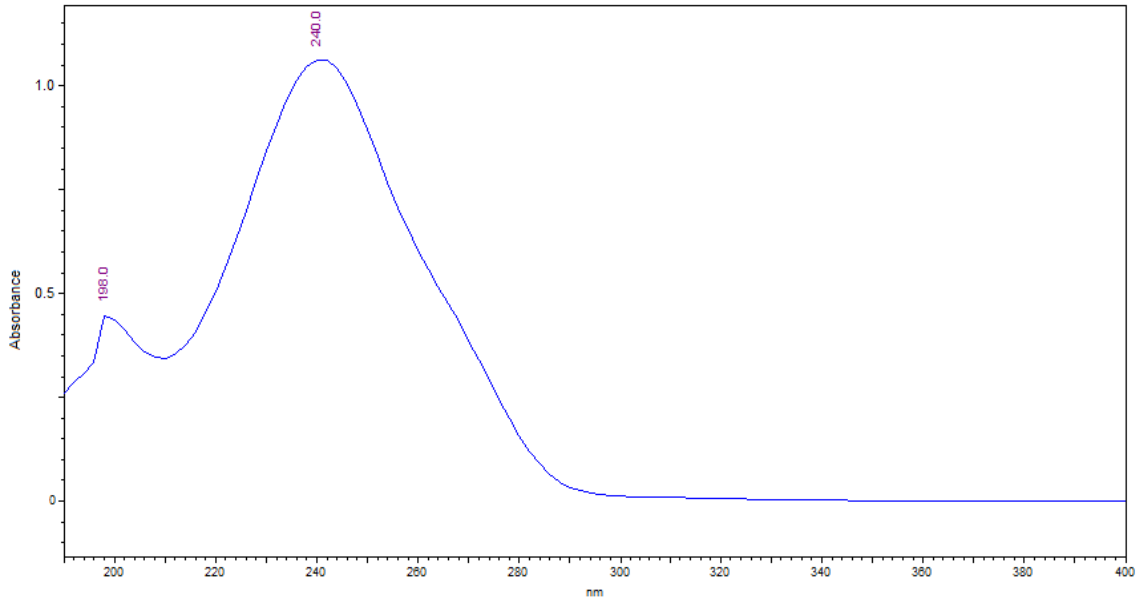

Figure 1: UV Spectrum of Terpineol

Based on the determined λmax (240 nm), a calibration curve was constructed using standard solutions of Terpineol with known concentrations ranging from 0 to 798.4 µg/mL. The absorbance values recorded at 240 nm for each concentration are presented in the table below:

Table 3: Absorbance of Terpineol for Calibration curve

Concentration (µg/mL)	Absorbance at 249 nm
0	0
159.68	0.012
319.36	0.025

479.04	0.038
638.72	0.051
798.4	0.062

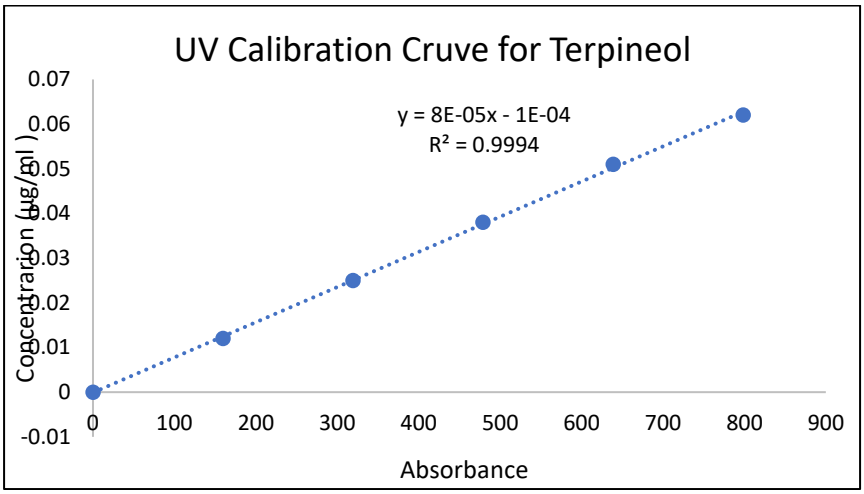

Figure 2: Calibration curve for Terpineol

The R^2 value of Calibration curve for Terpineol was found to be 0.999, these data obtained demonstrated a linear relationship between concentration and absorbance, validating the applicability of Beer-Lambert's law within the tested range. This calibration curve was subsequently used for the quantitative estimation of Terpineol in various formulations.

4.4. ATR-FTIR of Terpineol

The ATR-FTIR analysis of Terpineol was performed using a Fourier Transform Infrared (FTIR) spectrophotometer equipped with an Attenuated Total Reflectance (ATR) accessory.

Key peaks observed and their corresponding functional group assignments are as follows:

- Broad absorption band at ~3350 cm^{-1}
- C–H stretching vibrations at ~2950–2850 cm^{-1}
- Weak absorption around ~1640 cm^{-1}
- Sharp bands at ~1460 cm^{-1} and ~1375 cm^{-1}:
- C–O stretching vibration at ~1050–1100 cm^{-1}
- Fingerprint region (below 1000 cm^{-1})

The Results of ATR-FTIR of Terpineol are given below:

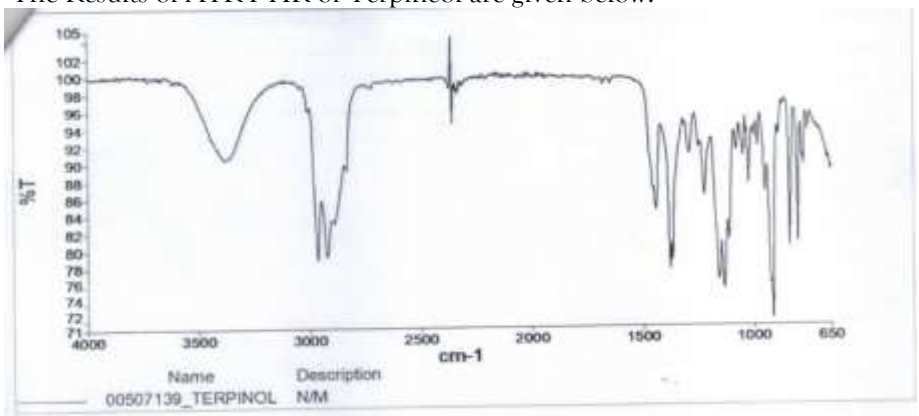

Figure 4: IR Spectrum of Terpineol

Key peaks in the IR spectrum of Terpineol include the stretching vibrations of following:

Table 4: Results of FTIR peak assignment for Terpineol based on the provided ATR-FTIR spectrum

Wavenumber (cm^{-1})	Peak Intensity	Functional Group	Vibrational Mode
~3350	Broad, strong	–OH (hydroxyl) group	O–H stretching
2950–2850	Medium	$–CH_3$, $–CH_2$ (alkyl groups)	C–H stretching
~1640	Weak to medium	C=C (alkene)	C=C stretching
~1460	Medium	$–CH_2$ (methylene)	C–H bending (scissoring)
~1375	Medium	$–CH_3$ (methyl)	C–H bending (wagging)
1100–1050	Medium to strong	C–O (alcohol)	C–O stretching
950–650	Complex, multiple	Various	C–H out-of-plane bending, ring modes

These IR spectral features confirm the structural integrity of terpineol, particularly the presence of hydroxyl, alkene, and alkyl functionalities. These peaks are identifying peaks for Terpineol. The obtained spectrums was compared to India Pharmacopoeia reference spectrum and significant similarity was observed.

4.5 NMR of Terpineol

The Nuclear Magnetic Resonance (NMR) analysis of Terpineol 1 (recorded at ~400 MHz in $CDCl_3$) confirms the presence of characteristic proton environments consistent with the structure of **α-terpineol**, a monoterpene alcohol with a cyclohexene backbone and an isopropyl group.

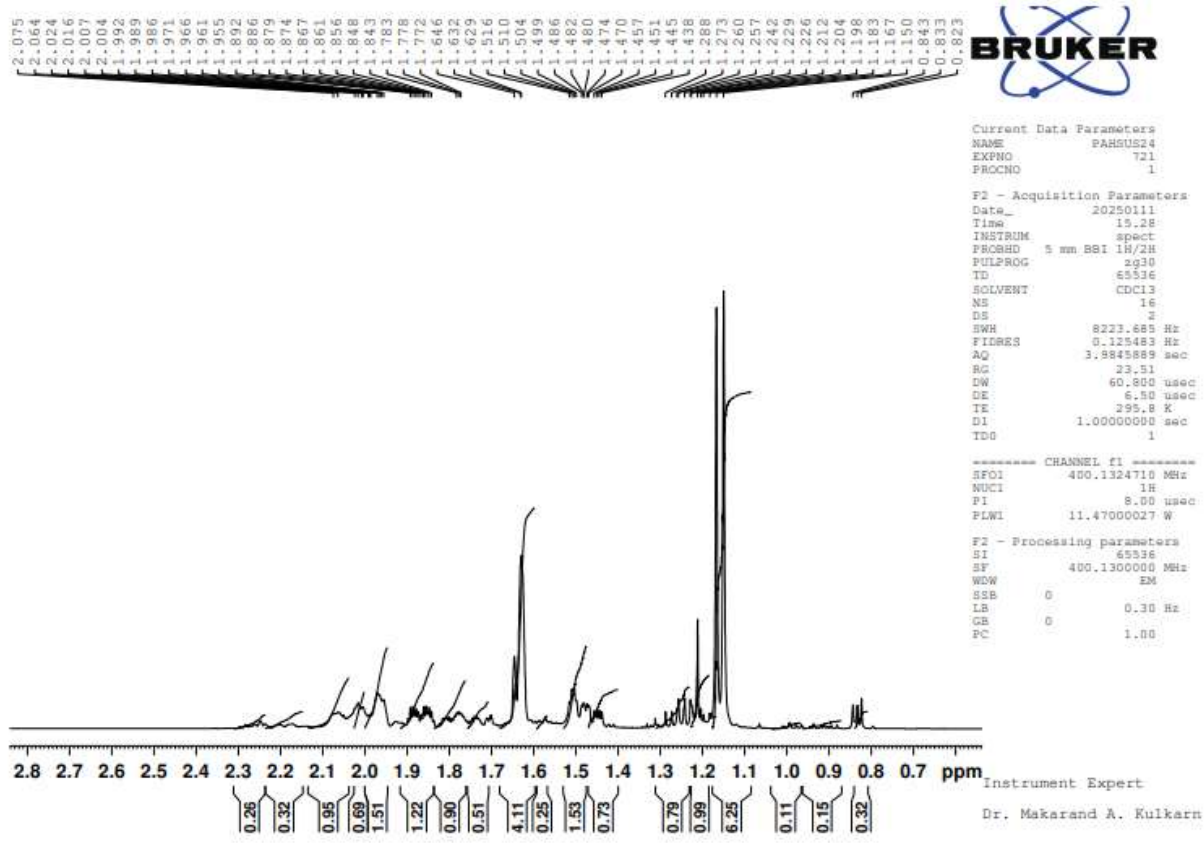

Figure 5 : NMR of Terpineol

The chemical shifts (δ, ppm), multiplicities, and peak assignments are described below:

International Journal of Environmental Sciences
ISSN: 2229-7359
Vol. 11 No. 18s, 2025
https://theaspd.com/index.php

Table 7.28: ^{1}H NMR Spectral Data of Terpineol ($CDCl_3$, 400 MHz)

δ (ppm)	Multiplicity	Integration	Proton Type / Environment	Assignment
~5.25	Multiplet	1H	Vinyl proton (olefinic proton)	=CH– (on cyclohexene ring)
~3.45	Multiplet	1H	Proton on carbon bearing –OH group	–CHOH
~1.70–2.10	Multiplet	2–3H	Allylic/benzylic protons (next to C=C)	CH_2 adjacent to double bond
~1.20–1.60	Multiplet	~6H	Cyclohexane ring protons	CH_2, CH (saturated ring positions)
~1.20	Singlet	3H	Methyl attached to the ring	CH_3– on ring
~0.90	Doublet	6H	Isopropyl methyl groups	$CH(CH_3)_2$

- The multiplet at ~5.25 ppm confirms the presence of a vinylic proton, a key feature of the cyclohexene ring in terpineol.
- The signal at ~3.45 ppm is indicative of a proton attached to a carbon bearing a hydroxyl group (–CHOH), characteristic of a secondary alcohol.
- The doublet at ~0.90 ppm, integrating for 6 protons, is assigned to two methyl groups of the isopropyl moiety.
- Multiplets between 1.2–2.1 ppm represent the complex aliphatic environment of the cyclohexene ring protons and nearby methylene groups.

Overall, the spectrum supports the structure of α-terpineol, with identifiable peaks for its hydroxyl group, alkene proton, isopropyl group, and alicyclic backbone.

The proton NMR spectrum of Terpineol 2 exhibits characteristic chemical shifts and splitting patterns that support its proposed structure—a monoterpene alcohol with a cyclic olefin and an isopropyl group.

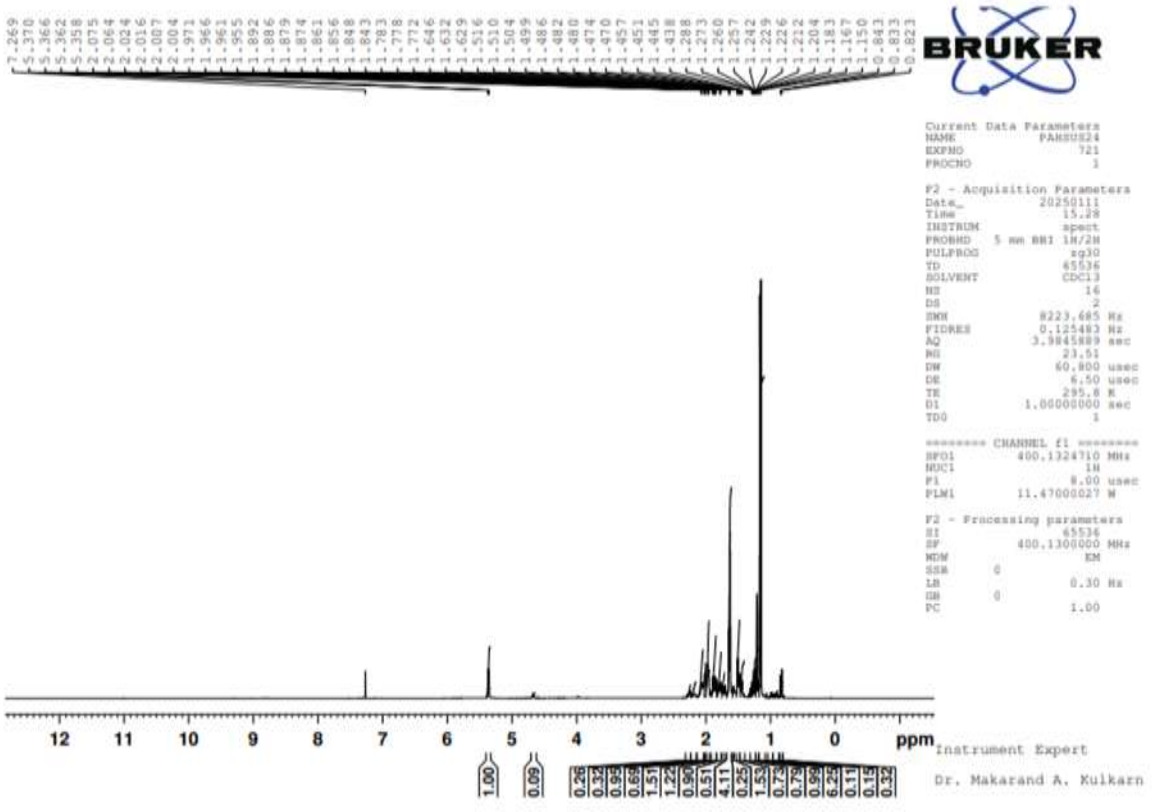

Figure 6: NMR of Terpineol 2

The chemical shifts (δ, ppm), multiplicities, and peak assignments are described below:

Table 5: ^{1}H NMR Chemical Shift Assignments for Terpineol (in $CDCl_3$)

Chemical Shift (δ, ppm)	Multiplicity	Integration	Type of Proton / Environment	Assignment
~5.20–5.30	Multiplet	1H	Vinylic proton	–CH= (on cyclohexene ring)
~3.40–3.50	Multiplet	1H	Proton on carbon bearing –OH	–CH(OH)– (secondary alcohol)
~1.60–2.10	Multiplet	2–3H	Allylic protons (next to C=C)	$–CH_2–$ adjacent to double bond
~1.20–1.60	Multiplet	~6H	Aliphatic ring protons	Cyclohexene CH_2/CH protons
~1.20	Singlet	3H	Methyl group attached to ring	$–CH_3$ (on saturated carbon of ring)
~0.90	Doublet	6H	Isopropyl methyl groups	$–CH(CH_3)_2$

- The vinylic proton appears as a multiplet at ~5.2–5.3 ppm, indicating the presence of an alkene within a cyclohexene ring system.
- A signal at ~3.4–3.5 ppm corresponds to a methine proton (–CHOH), confirming the hydroxyl substitution on the ring—typical for a secondary alcohol.
- The doublet at ~0.90 ppm, integrating for 6H, matches well with two methyl groups of an isopropyl moiety, which is consistent with the side chain in Terpineol.
- The aliphatic and ring protons result in multiplets between 1.2–2.1 ppm, representing the complex environment of methylene and methine protons in a substituted cyclohexene ring.
- No aromatic or acidic protons are observed, consistent with the aliphatic structure of Terpineol.

These spectral features fully support the expected structure of **α-terpineol**, validating its identity and purity.

4.7. Purity Study by gas Chromatography

The gas chromatographic analysis of the α-terpineol sample revealed a dominant peak at a retention time of 10.276 minutes, which corresponds to α-terpineol and accounted for 80.28% of the total peak area. This indicates that α-terpineol is the major component present in the sample and suggests high chemical purity. In addition to the primary peak, several smaller peaks were detected at retention times ranging from 7.44 to 11.88 minutes, each contributing between 0.44% and 4.86% of the total area. These minor peaks likely represent structurally related terpenoids or trace impurities such as β-terpineol, terpinen-4-ol, or other monoterpene derivatives.

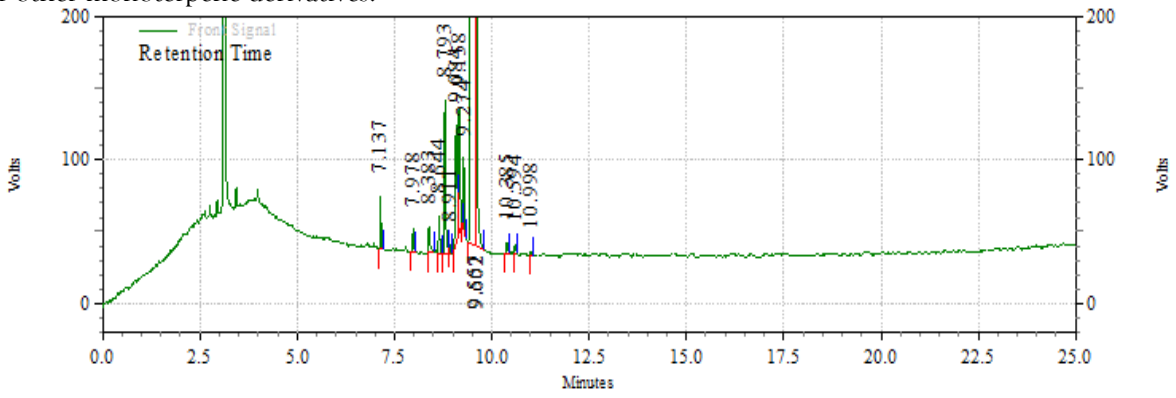

Figure 7: Chromatogram of Terpineol

The GC profile thus confirms that the sample predominantly contains α-terpineol, with minimal contamination, supporting its suitability for further application in pharmaceutical or aromatic formulations.

4.8. Drug-Excipient compatibility study

To assess the compatibility of Terpineol with various excipients and vehicles, respectiv mixtures were stored at 50 °C for a period of four weeks. Following this, the Terpineol content was analyzed using a UV-Visible spectrophotometer. The percentage assay and absorbance values of Terpineol across different prototypes are presented below:

Table 7: Drug-Excipient compatibility study by UV Spectrophotometer

Prototypes	%Assay	Absorbance
EC1	95.78	0.243
EC2	96.84	0.247
EC3	**99.29**	**0.251**
EC4	96.21	0.248
EC5	98.06	0.249
EC6	**99.91**	**0.254**

Based on the % assay results, Terpineol demonstrated compatibility with all six excipients tested. However, it exhibited notably higher compatibility with Chitosan (EC3) and Sodium Tripolyphosphate (EC6) in comparison to the other excipients. Among the prototypes, EC6 exhibited the highest Terpineol content with a % assay of 99.91% and an absorbance of 0.254, suggesting excellent compatibility and minimal loss during the storage period. Similarly, EC3 also demonstrated high stability, with a % assay of 99.29% and absorbance of 0.251, further supporting the robustness of the formulation in that combination.

The remaining prototypes—EC2 (96.84%), EC4 (96.21%), and EC5 (98.06%)—also maintained Terpineol content close to the theoretical value, indicating acceptable stability and no significant interaction with their respective excipients. EC1, with a slightly lower assay value of 95.78% and absorbance of 0.243, still fell within an acceptable range, though it may indicate a marginally higher degree of interaction or degradation compared to other formulations.

Their purity and compatibility was subsequently evaluated using FTIR, and the results are presented below.

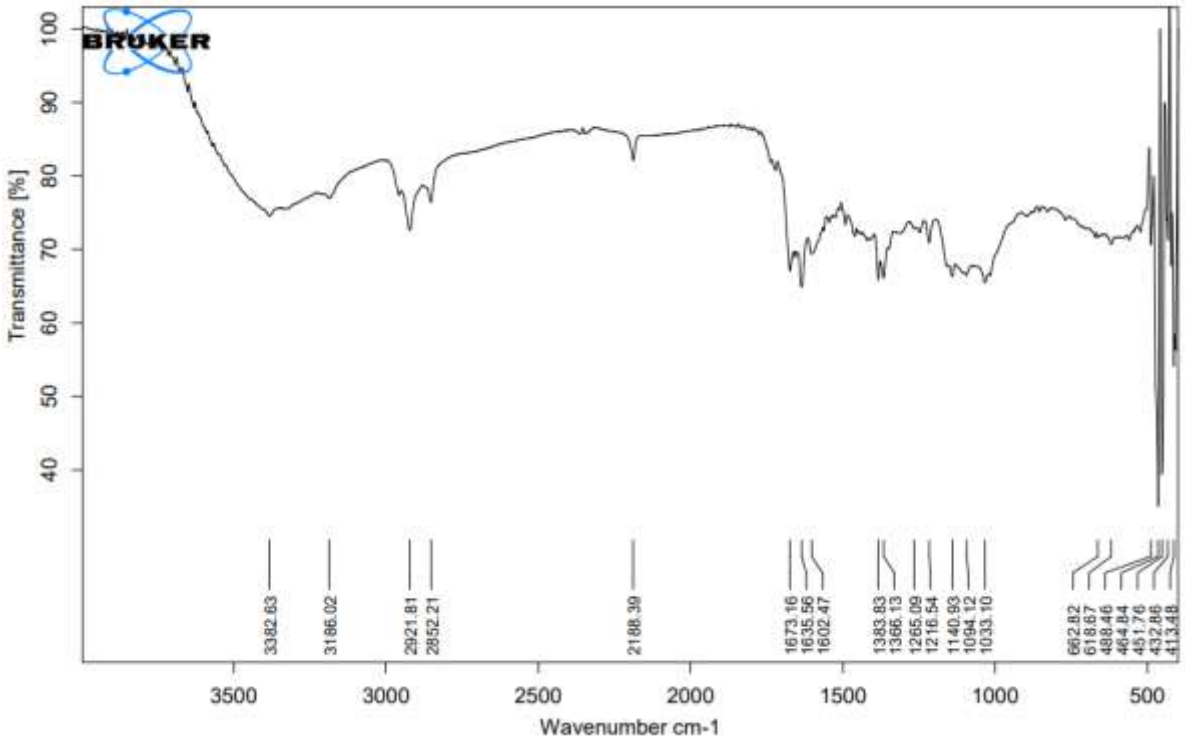

Figure 7.30: FTIR of Chitosan

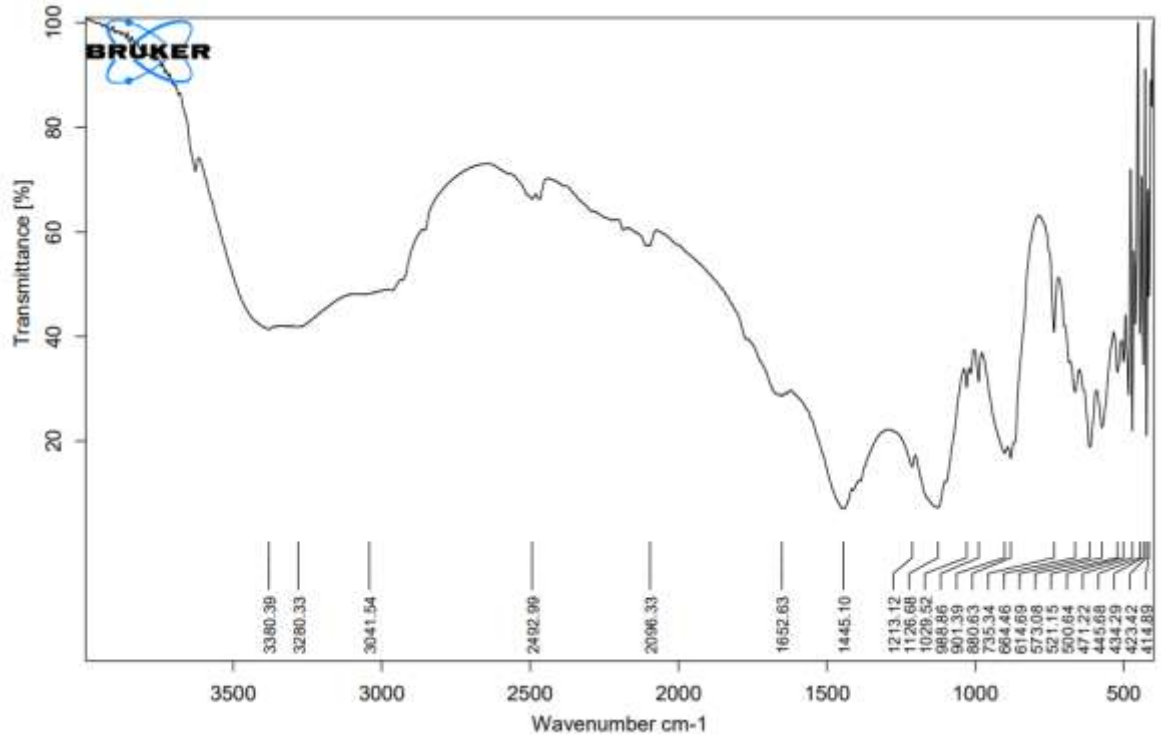

Figure 8: FTIR of STPP

These peaks are identifying peaks for Terpineol. There were no significant difference found when spectrums were compared to India Pharmacopoeia reference spectrum and Standard spectrum. Hence, Terpineol was found compatible with selected excipients.

: All formulations were visually observed to be milky white, uniform emulsions without visible phase separation immediately after preparation then the formulation was evaluated for globule size and zeta potential. The variation in the type and amount of polymer, oil, and surfactant among the prototypes was intended to evaluate their influence on the nanocapsule characteristics, particularly globule size and zeta potential.

Formulation and Optimization of TNC Using Design Expert

The optimization of Terpineol nanocapsules was done by using Design Expert 13 software using Randomized Central Composite Response surface model.

DESIGN EXPERT STUDIES – TERPINEOL

Table 9: Build Information

File Version	13.0.5.0		
Study Type	Response Surface	**Subtype**	Randomized
Design Type	Central Composite	**Runs**	9.00
Design Model	Quadratic	**Blocks**	No Blocks

Table 10: Factors

Factor	Name	Units	Type	SubType	Minimum	Maximum	Coded Low	Coded High	Mean	Std. Dev.

A	Chitosan Conc	mg	Numeric	Continuous	300.00	500.00	-1 ↔ 300.00	+1 ↔ 500.00	400.00	86.60
B	STPP Conc	mg	Numeric	Continuous	50.00	150.00	-1 ↔ 50.00	+1 ↔ 150.00	100.00	43.30

Table 11: Responses

Response	Name	Units	Observations	Minimum	Maximum	Mean	Std. Dev.	Ratio
R1	Particle Size	nm	9.00	93.4	309.3	188.20	90.21	3.31
R2	Entrapment Efficiency	%	9.00	66.05	77.56	71.52	4.33	1.17

Table 12: ACTUAL DESIGN

	Factor 1	Factor 2	Response 1
Run	A:Chitosan Conc	B:STPP Conc	Particle Size
	Mg	mg	nm
1	400	100	159.8
2	400	50	171.3
3	400	150	166.3
4	300	50	101.1
5	500	150	309.3
6	300	100	93.4
7	500	50	301.7
8	300	150	97.2
9	500	100	293.7

RESPONSE 1
PARTICLE SIZE
Fit Summary
Response 1: Particle Size

Source	Sequential p-value	Lack of Fit p-value	Adjusted R^2	Predicted R^2	
Linear	< 0.0001		0.9493	0.9181	
2FI	0.8051		0.9400	0.8271	
Quadratic	**0.0012**		**0.9989**	**0.9948**	**Suggested**
Cubic	0.0284		1.0000	0.9999	**Aliased**

Sequential Model Sum of Squares [Type I]
Response 1: Particle Size

Source	Sum of Squares	df	Mean Square	F-value	p-value	
Mean vs Total	3.188E+05	1	3.188E+05			
Linear vs Mean	62628.45	2	31314.22	75.90	< 0.0001	
2FI vs Linear	33.06	1	33.06	0.0677	0.8051	
Quadratic vs 2FI	**2414.57**	**2**	**1207.28**	**129.98**	**0.0012**	**Suggested**
Cubic vs Quadratic	27.84	2	13.92	618.70	0.0284	Aliased
Residual	0.0225	1	0.0225			
Total	3.839E+05	9	42653.01			

Quadratic vs 2FI is the highest order polynomial where the additional terms are significant and the model is not aliased.

Model Summary Statistics

Source	Std. Dev.	R^2	Adjusted R^2	Predicted R^2	PRESS	
Linear	20.31	0.9620	0.9493	0.9181	5332.13	
2FI	22.10	0.9625	0.9400	0.8271	11256.46	
Quadratic	**3.05**	**0.9996**	**0.9989**	**0.9948**	**339.59**	**Suggested**
Cubic	0.1500	1.0000	1.0000	0.9999	4.10	Aliased

Quadratic model maximizing the **Adjusted R^2** and the **Predicted R^2**.
The **Model F-value** of 1401.29 implies the model is significant. There is only a 0.01% chance that an F-value this large could occur due to noise.
P-values less than 0.0500 indicate model terms are significant. In this case A, A^2, B^2 are significant model terms. Values greater than 0.1000 indicate the model terms are not significant. If there are many insignificant model terms (not counting those required to support hierarchy), model reduction may improve your model.

Final Equation in Terms of Coded Factors
Particle Size =+159.90+102.17A-0.2167B+2.87AB+33.60A^2+8.85B^2
The high levels of the factors are coded as +1 and the low levels are coded as -1.

Final Equation in Terms of Actual Factors
Particle Size =+347.66667-1.72383Chitosan Conc-0.942333STPP Conc+0.000575Chitosan Conc * STPP Conc+0.003360Chitosan $Conc^2$+0.003540STPP $Conc^2$
The equation in terms of actual factors can be used to make predictions about the response for given levels of each factor.

Table 13: Particle size Report

Run Order	Actual Value	Predicted Value	Residual	Leverage	Internally Studentized Residuals	Externally Studentized Residuals	Cook's Distance	Influence on Fitted Value DFFITS	Standard Order
1	159.80	159.90	-0.1000	0.556	-0.049	-0.040	0.001	-0.045	9
2	171.30	168.97	2.33	0.556	1.148	1.253	0.275	1.400	7
3	166.30	168.53	-2.23	0.556	-1.099	-1.161	0.252	-1.298	8

4	101.10	103.27	-2.17	0.806	-1.618	-3.710	1.809(1)	-7.551(1)	1
5	309.30	307.18	2.13	0.806	1.581	3.164	1.726(1)	6.439(1)	4
6	93.40	91.33	2.07	0.556	1.017	1.026	0.216	1.147	5
7	301.70	301.86	-0.1583	0.806	-0.118	-0.096	0.010	-0.196	2
8	97.20	97.09	0.1083	0.806	0.081	0.066	0.004	0.134	3
9	293.70	295.67	-1.97	0.556	-0.968	-0.953	0.195	-1.066	6

ACTUAL VS PREDICTED GRAPH

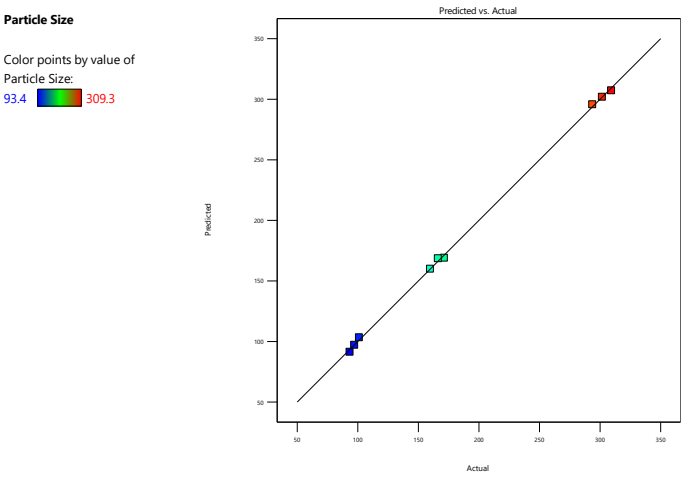

Figure 8: Actual vs Predicted plot for PS of TPNCs

The Predicted vs. Actual plot for the particle size of Terpineol-loaded nanocapsules demonstrates a strong correlation between the experimentally observed and statistically predicted values, indicating the reliability and accuracy of the formulation model. The data points closely align along the diagonal line (y = x), which confirms that the model used for optimization effectively predicted the particle size across the tested formulation conditions. The color gradient ranging from blue (smaller particle sizes around 93.4 nm) to red (larger sizes up to 309.3 nm) further visualizes the distribution of particle sizes and supports the consistency of the results.

CONTOUR

International Journal of Environmental Sciences
ISSN: 2229-7359
Vol. 11 No. 18s, 2025
https://theaspd.com/index.php

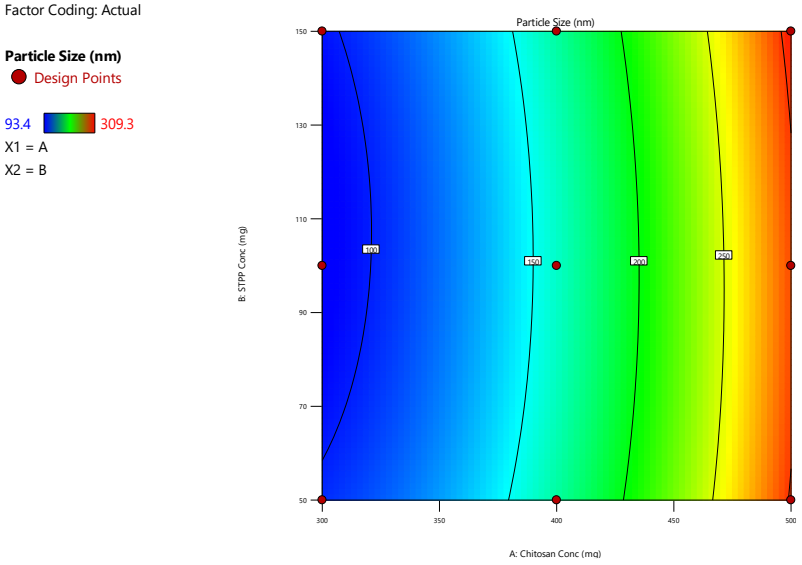

Figure 9: Contour plot for PS of TPNCs

3D SURFACE PLOT

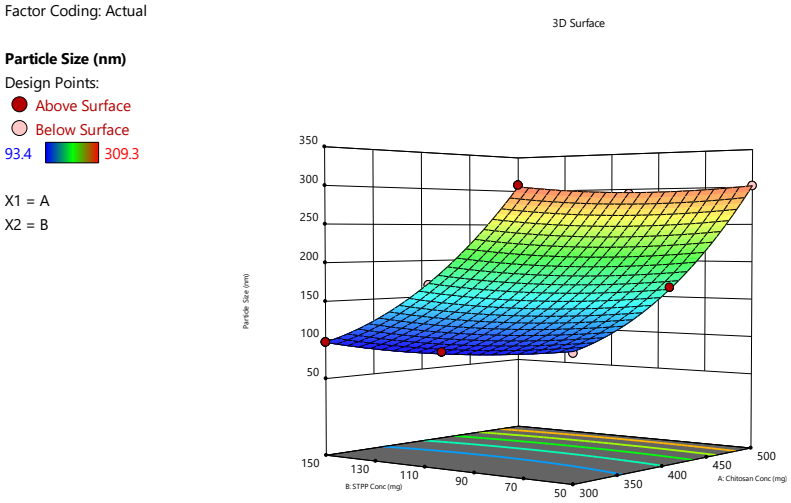

Figure 10: 3D Surface plot for PS of TPNCs

The 3D surface plot illustrates the interactive effect of Chitosan concentration (X1) and Sodium Tripolyphosphate (STPP) concentration (X2) on the particle size of Terpineol-loaded nanocapsules. The surface is color-coded, ranging from blue (indicating smaller particle sizes around 93.4 nm) to red (larger sizes up to 309.3 nm). The shape and gradient of the surface suggest that both chitosan and STPP concentrations positively influence particle size, with the effect being more pronounced for chitosan.

RESPONSE 2

ENTRAPMENT EFFICIENCY

Table 14: ACTUAL DESIGN

	Factor 1	Factor 2	Response 2
Run	A:Chitosan Conc	B:STPP Conc	Entrapment Efficiency
	mg	mg	%
1	400	100	74.29
2	400	50	77.56
3	400	150	66.78
4	300	50	74.88
5	500	150	67.76
6	300	100	69.81

7	500	50	76.36
8	300	150	66.05
9	500	100	70.17

Fit Summary

Response 2: Entrapment Efficiency

Source	Sequential p-value	Lack of Fit p-value	Adjusted R^2	Predicted R^2	
Linear	0.0011		0.8632	0.8285	**Suggested**
2FI	0.9503		0.8359	0.7838	
Quadratic	0.3096		0.8749	0.5899	
Cubic	0.8521		0.7275	-5.2090	**Aliased**

Sequential Model Sum of Squares [Type I]

Response 2: Entrapment Efficiency

Source	Sum of Squares	df	Mean Square	F-value	p-value	
Mean vs Total	46033.13	1	46033.13			
Linear vs Mean	134.73	2	67.37	26.23	0.0011	**Suggested**
2FI vs Linear	0.0132	1	0.0132	0.0043	0.9503	
Quadratic vs 2FI	8.35	2	4.17	1.78	0.3096	
Cubic vs Quadratic	1.93	2	0.9649	0.1886	0.8521	**Aliased**
Residual	5.12	1	5.12			
Total	46183.28	9	5131.48			

Linear vs Mean is the highest order polynomial where the additional terms are significant and the model is not aliased.

Model Summary Statistics

Source	Std. Dev.	R^2	Adjusted R^2	Predicted R^2	PRESS	
Linear	**1.60**	**0.8974**	**0.8632**	**0.8285**	**25.75**	**Suggested**
2FI	**1.75**	**0.8975**	**0.8359**	**0.7838**	**32.46**	
Quadratic	**1.53**	**0.9531**	**0.8749**	**0.5899**	**61.58**	
Cubic	**2.26**	**0.9659**	**0.7275**	**-5.2090**	**932.23**	**Aliased**

Linear model maximizing the Adjusted R^2 and the Predicted R^2.

ANOVA for Linear model

Response 2: Entrapment Efficiency

Source	Sum of Squares	Df	Mean Square	F-value	p-value	
Model	134.73	2	67.37	26.23	0.0011	**significant**
A-Chitosan Conc	2.10	1	2.10	0.8179	0.4006	
B-STPP Conc	132.63	1	132.63	51.65	0.0004	
Residual	15.41	6	2.57			
Cor Total	150.14	8				

Factor coding is Coded.

Sum of squares is Type III - Partial

The Model F-value of 26.23 implies the model is significant. There is only a 0.11% chance that an F-value this large could occur due to noise.

P-values less than 0.0500 indicate model terms are significant. In this case B is a significant model term.

Values greater than 0.1000 indicate the model terms are not significant. If there are many insignificant

model terms (not counting those required to support hierarchy), model reduction may improve your model.

Fit Statistics

Std. Dev.	1.60		**R^2**	0.8974
Mean	71.52		**Adjusted R^2**	0.8632
C.V. %	2.24		**Predicted R^2**	0.8285
			Adeq Precision	11.4426

The Predicted R^2 of 0.8285 is in reasonable agreement with the Adjusted R^2 of 0.8632; i.e. the difference is less than 0.2.

Adeq Precision measures the signal to noise ratio. A ratio greater than 4 is desirable. Your ratio of 11.443 indicates an adequate signal. This model can be used to navigate the design space.

Model Comparison Statistics

PRESS	25.75
-2 Log Likelihood	30.38
BIC	36.97
AICc	41.18

Coefficients in Terms of Coded Factors

Factor	Coefficient Estimate	df	Standard Error	95% CI Low	95% CI High	VIF
Intercept	71.52	1	0.5342	70.21	72.82	
A-Chitosan Conc	0.5917	1	0.6542	-1.01	2.19	1.0000
B-STPP Conc	-4.70	1	0.6542	-6.30	-3.10	1.0000

The coefficient estimate represents the expected change in response per unit change in factor value when all remaining factors are held constant. The intercept in an orthogonal design is the overall average response of all the runs. The coefficients are adjustments around that average based on the factor settings. When the factors are orthogonal the VIFs are 1; VIFs greater than 1 indicate multi-colinearity, the higher the VIF the more severe the correlation of factors. As a rough rule, VIFs less than 10 are tolerable.

Final Equation in Terms of Coded Factors

Entrapment Efficiency = +71.52+0.5917A-4.70B

The high levels of the factors are coded as +1 and the low levels are coded as -1.

Final Equation in Terms of Actual Factors

Entrapment Efficiency =+78.55444+0.005917Chitosan Conc-0.094033STPP Conc

The equation in terms of actual factors can be used to make predictions about the response for given levels of each factor.

Table 15: Report of Entrapment Efficiency of TPNCs

Run Order	Actual Value	Predicted Value	Residual	Leverage	Internally Studentized Residuals	Externally Studentized Residuals	Cook's Distance	Influence on Fitted Value DFFITS	Standard Order
1	74.29	71.52	2.77	0.111	1.835	2.528	0.140	0.894	9
2	77.56	76.22	1.34	0.278	0.984	0.981	0.124	0.609	7
3	66.78	66.82	-0.0361	0.278	-0.027	-0.024	0.000	-0.015	8

4	74.88	75.63	-0.7478	0.444	-0.626	-0.591	0.105	-0.529	1
5	67.76	67.41	0.3522	0.444	0.295	0.271	0.023	0.243	4
6	69.81	70.93	-1.12	0.278	-0.820	-0.794	0.086	-0.492	5
7	76.36	76.81	-0.4511	0.444	-0.378	-0.349	0.038	-0.312	2
8	66.05	66.22	-0.1744	0.444	-0.146	-0.134	0.006	-0.119	3
9	70.17	72.11	-1.94	0.278	-1.424	-1.598	0.260	-0.991	6

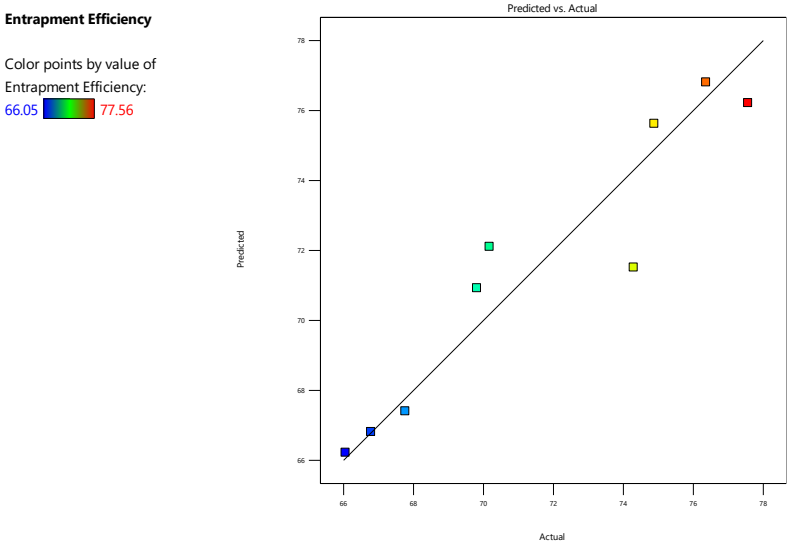

Figure 11: Actual vs Predicted plot for EE of TPNCs

These results imply that the selected factors—chitosan and STPP concentrations—are significant contributors to the entrapment efficiency of Terpineol, with the model successfully capturing their effects. This reinforces the robustness of the formulation design and supports the reliability of the optimization approach for achieving high drug loading efficiency.

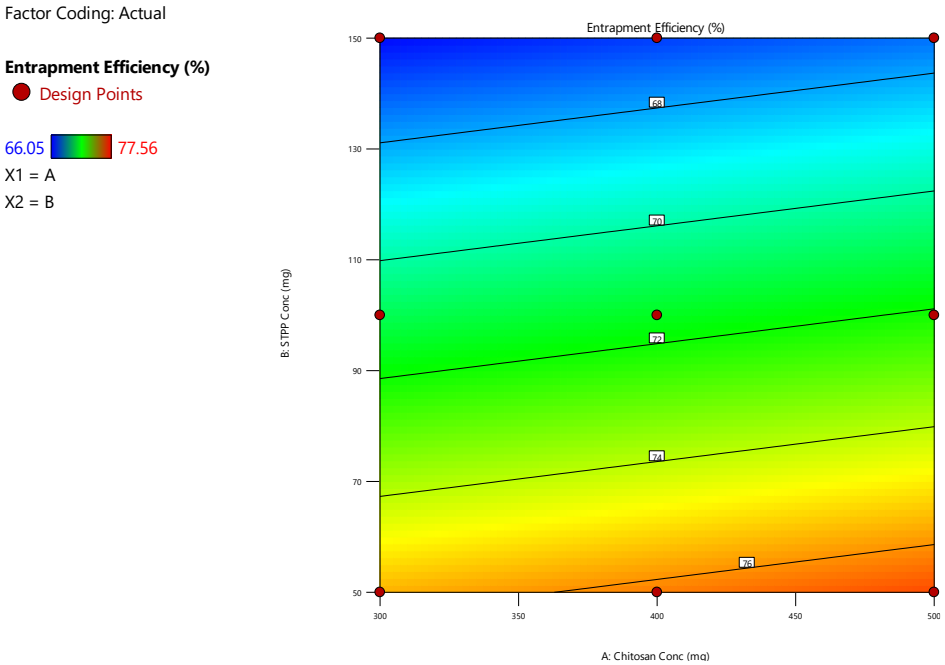

Figure 12: Contour plot for EE of TPNCs

The contour plot clearly illustrates the combined effect of chitosan (X1) and STPP (X2) concentrations on the entrapment efficiency of Terpineol in chitosan nanocapsules. As observed, the entrapment efficiency increases progressively from the top-left (blue) to the bottom-right (red) region of the plot, indicating that higher concentrations of both chitosan and STPP lead to improved drug entrapment. The

trend suggests a synergistic effect between the polymer and crosslinker, where increasing chitosan enhances the matrix density for drug incorporation, while higher STPP promotes more effective rosslinking, stabilizing the encapsulated drug.

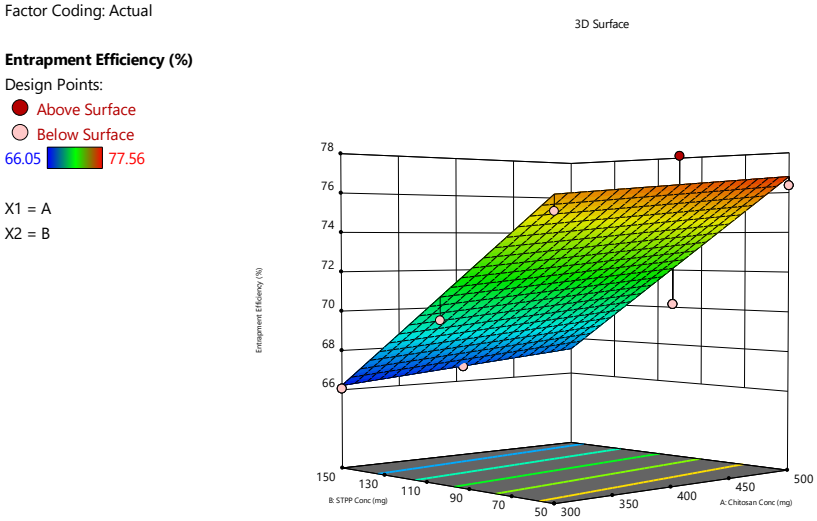

Figure 13: 3D Surface plot for EE of TPNCs

Increasing both chitosan and STPP concentrations positively influences entrapment efficiency. This is likely due to enhanced ionic cross-linking between the amino groups of chitosan and phosphate groups of STPP, leading to better encapsulation of the active substance. The model predicts the behavior well, and this surface plot is valuable for optimizing formulation conditions.

7.5 Evaluation of Terpineol Nanocapsules

The prepared Terpineol-loaded nanocapsules were evaluated based on various physicochemical, morphological, and structural parameters as described below:

a. Physical Appearance:

The TPNCs 9 formulations were dried and nanocapsules appeared as a fine, off-white to yellow, free-flowing powder with uniform texture and no visible aggregation or discoloration. The formulation was stable with no signs of moisture-induced clumping.

The results are given below:

Table 15: Physical Appearance evaluations of MENCs

Prototype	Physical Appearance
F1	off white to slightly Yellow Amorphous powder
F2	off white to slightly Yellow Amorphous powder
F3	off white to slightly Yellow Amorphous powder
F4	off white to slightly Yellow Amorphous powder
F5	off white to slightly Yellow Amorphous powder
F6	off white to slightly Yellow Amorphous powder
F7	off white to slightly Yellow Amorphous powder
F8	off white to slightly Yellow Amorphous powder
F9	off white to slightly Yellow Amorphous powder

b. pH Measurement

The pH of the 9 prototypes of nanoscapsules was measured by using a pH meter. The sample was taken in a beaker and the electrode of the pH meter was dipped inside the formulation and the pH reading displayed was noted down.

The results of pH were given in table below:

Table 16: Results of pH of Nanosuspension

Sr. No.	Prototype	pH
1.	F1	4.76
2.	F2	4.77
3.	F3	4.83
4.	F4	4.80
5.	F5	4.82
6.	F6	4.76
7.	F7	4.78
8.	F8	4.79
9.	F9	4.76

c. Active Content Determination

The active content of Terpineol in the prepared nanocapsules was successfully quantified using UV-Visible spectrophotometry at an absorbance maximum of 240 nm. The Nanocapsules dispersion was appropriately diluted with methanol, and absorbance was measured against a reagent blank.

Table 17: Results of Active Content Determination

Sr. No.	Prototype	Drug Content (%)
1.	F1	92.09 ± 1.19
2.	F2	93.16 ± 1.91
3.	F3	90.19 ± 0.86
4.	F4	95.23 ± 0.51
5.	F5	91.72 ± 1.91
6.	**F6**	**96.72 ± 2.83**
7.	F7	93.90 ± 1.84
8.	F8	92.49 ± 0.67
9.	F9	91.61 ± 0.49

The active drug content of terpineol nanocapsule formulations ranged from 90.19% to 96.72%, indicating effective incorporation of terpineol within the nanocarrier matrix. F6 exhibited the highest active drug content (96.72 ± 2.83%), suggesting optimal formulation conditions that favored maximum drug loading. This was closely followed by F4 (95.23 ± 0.51%) and F7 (93.90 ± 1.84%), which also demonstrated efficient incorporation. In contrast, F3 showed the lowest drug content (90.19 ± 0.86%), possibly due to formulation variables that may have limited drug retention during preparation. Most other formulations, including F1, F2, F5, F8, and F9, presented drug content values within a narrow and acceptable range (approximately 91–93%), indicating reproducibility of the interfacial deposition method

d. Particle size

The particle size of the 9 prototypes of nanoscapsules was measured and the results of are given in table below:

Table 18: Results of Particle size

Sr. No.	Prototype	Particle size (nm)
1.	F1	159.8 ± 26.7
2.	F2	171.3 ± 25.3
3.	F3	166.3 ± 12.9
4.	F4	190.1 ± 17.3
5.	F5	309.3 ± 21.9
6.	**F6**	**93.4 ± 18.6**

7.	F7	301.7 ± 22.3
8.	F8	197.2 ± 25.9
9.	F9	293.7 ± 13.7

The particle size analysis of the terpineol nanocapsule formulations revealed a broad range from 93.4 nm to 309.3 nm, indicating the influence of formulation variables such as polymer and crosslinker concentration. Among all, F6 exhibited the smallest particle size (93.4 ± 18.6 nm). These smaller sizes are favorable for enhanced bioavailability and cellular uptake. On the other hand, F5 (309.3 ± 21.9 nm), F7 (301.7 ± 22.3 nm), and F9 (293.7 ± 13.7 nm) showed significantly larger particle sizes, which may be due to higher polymer content or suboptimal crosslinking leading to particle aggregation. The intermediate sizes observed in F1, F2, F3 & F4 (ranging from ~159 to ~197.2 nm) suggest a relatively balanced formulation. Overall, the results highlight that F6 is the most promising formulations in terms of achieving nanoscale size with good uniformity, which is critical for effective drug delivery.

e. Zeta potential

The particle size of the 9 prototypes of nanoscapsules was measures and the results of are given in table below

Table 19: Results of Zeta potential

Sr. No.	Prototype	Zeta Potential (mV)
1.	F1	-17.2
2.	F2	-15.9
3.	F3	-16.4
4.	**F4**	**-21.6**
5.	F5	-9.2
6.	**F6**	**-26.7**
7.	F7	-11.6
8.	**F8**	**-24.3**
9.	F9	-12.3

The zeta potential values of the terpineol nanocapsule formulations ranged from –9.2 mV to –26.7 mV, reflecting the surface charge and colloidal stability of the nanosystems. F6 exhibited the highest negative zeta potential (–26.7 mV), followed by F8 (–24.3 mV) and F4 (–21.6 mV), indicating strong electrostatic repulsion between particles and enhanced formulation stability. A more negative zeta potential generally reduces the likelihood of particle aggregation, promoting a stable nanosuspension. In contrast, F5 (–9.2 mV), F7 (–11.6 mV), and F9 (–12.3 mV) showed the lowest negative zeta potential values, suggesting reduced stability and a higher risk of particle aggregation over time.

g. DSC

Based on above evaluations the DSC of TPNC F6 was performed and the results are given below:

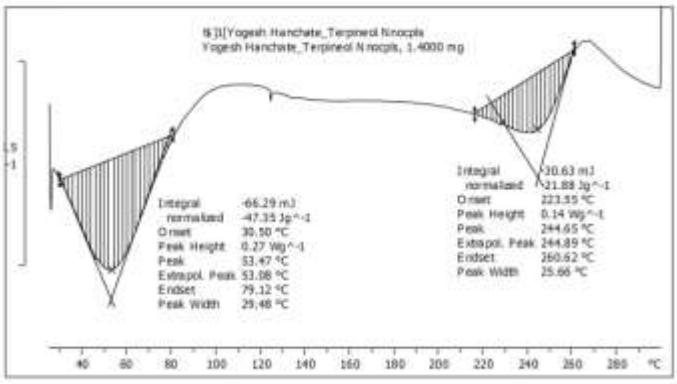

Figure 15 : DSC of TPNC -6

The DSC thermogram of terpineol nanocapsules exhibited two distinct endothermic transitions. The first peak, observed at 53.47 °C, corresponds to the melting or glass transition of the polymer matrix and the encapsulated terpineol. This transition suggests that terpineol is effectively incorporated in an amorphous or partially crystalline form within the nanocapsule system. The second endothermic event, peaking at 244.65 °C, likely represents the decomposition or thermal degradation of the polymer and/or terpineol-loaded matrix. This higher temperature transition with a lower enthalpy change (–21.88 J/g) indicates that the system remains thermally stable up to this temperature, which is advantageous for storage and handling of the formulation.

Overall, the absence of a sharp melting endotherm for pure terpineol and the presence of a broad peak in the nanocapsule formulation confirm successful encapsulation and reduced crystallinity, which are desirable for enhancing solubility, stability, and bioavailability of the active compound.

h. SEM

Surface morphology of TP Nanocapsules was examined by scanning electron microscopy. The SEM images of Batch F6 was scanned for SEM and its figures are given below. SEM analysis showed that the prepared Nanocapsules were having size in nanometers and the particles were nearly spherical.

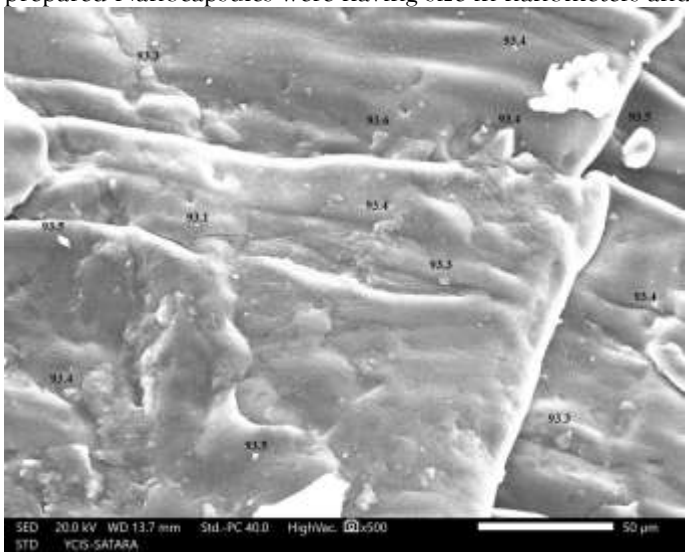

Figure 16: SEM Images of TP Nanocapsules of formulation F6

i. Entrapment Efficiency

The drug entrapment efficiency for TPNCs all formulations performed and the results are given below:

Table 20: Results of Entrapment Efficiency

Sr. No.	Prototype	Entrapment Efficiency (%)
1.	F1	59.29 ± 0.42
2.	F2	62.46 ± 0.63
3.	F3	54.78 ± 0.81
4.	F4	59.88 ± 0.38
5.	F5	52.76 ± 0.46
6.	**F6**	**84.81 ± 0.73**
7.	F7	61.36 ± 0.98
8.	F8	51.05 ± 1.03
9.	F9	55.17 0.19

The entrapment efficiency (EE) of the terpineol nanocapsule formulations varied from 51.05% to 84.81%, indicating a moderate encapsulation capacity across all prototypes. The highest EE was observed in F6 84.81% ± 0.73% suggesting that these formulations had a favorable balance between polymer concentration and crosslinking density, enabling better drug incorporation within the nanocapsule

matrix. In contrast, F8 (51.05 ± 1.03%) and F5 (52.76 ± 0.46%) showed the lowest EE, potentially due to insufficient interaction between the drug and polymer or possible drug leakage during preparation. The remaining formulations (F1,F2, F3,F4, F7, and F9) showed EE values between 54% and 59%, which are within an acceptable range for nanocarrier systems but less efficient compared to F2.

7.8 In-vitro studies using Dialysis Bag study

The in-vitro drug release profile of the terpineol nanocapsules (TNC-6) demonstrated a sustained and time-dependent release over 12 hours (720 minutes)

The data reflects a sustained release behavior, which is desirable for prolonged therapeutic action, minimizing frequent dosing. The square root of time and log-transformed data suggest that the release kinetics may fit Higuchi or Korsmeyer-Peppas models, indicating diffusion-controlled or anomalous transport mechanisms.

Table 21 :In -vitro studies of TNC-6

verall, the results confirm that the formulated terpineol nanocapsules effectively prolong drug release, making them suitable for applications requiring extended delivery, such as in anti-inflammatory or .

Terpineol NC in-vitro drug release study TNC-06				
Time (min.)	Sqrt of Time	Log of Time	% DR	Log % DR
0.00	0.00	0.00	0.00	0.00
60.00	7.75	1.78	8.11	0.91
120.00	10.95	2.08	17.36	1.24
240.00	15.49	2.38	35.19	1.55
360.00	18.97	2.56	51.12	1.71
480.00	21.91	2.68	68.19	1.83
720.00	26.83	2.86	88.37	1.95

Figure 7.42: Zero order release kinetics for TNC

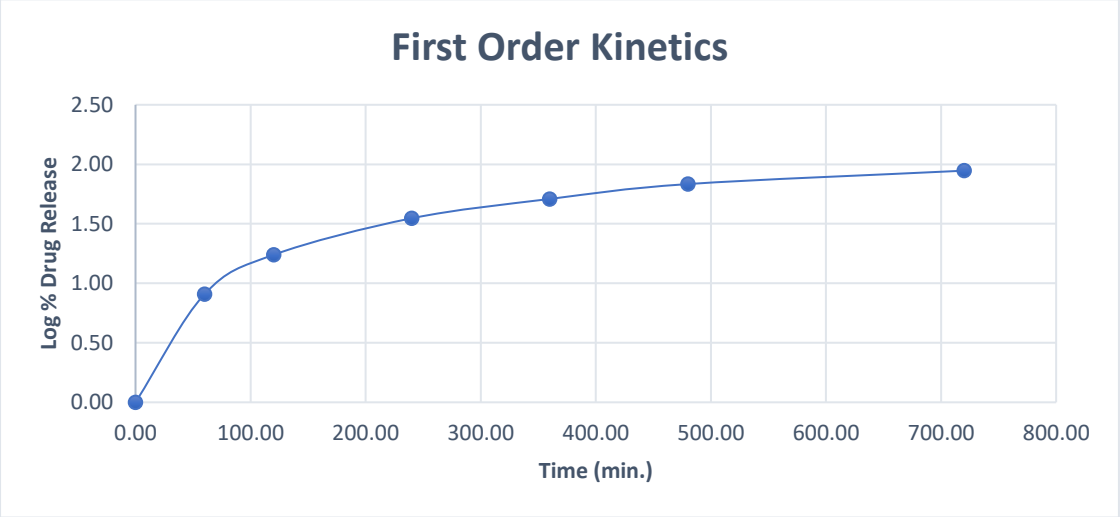

Figure 7.43: First order release kinetics for TNC

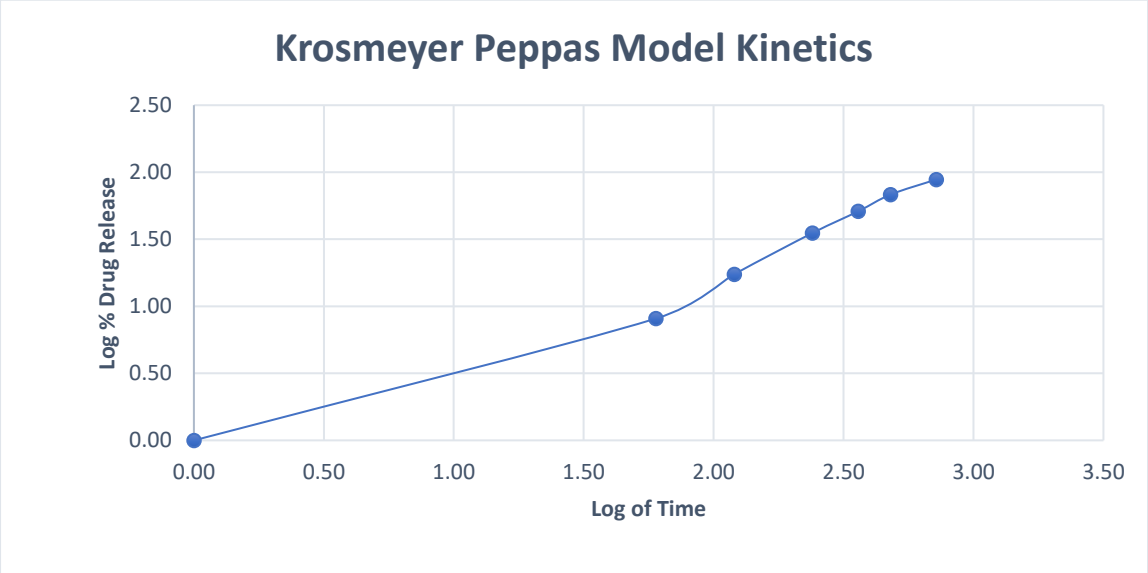

Figure 7.44: Krosmeyer Peppas release kinetics for TNC-04

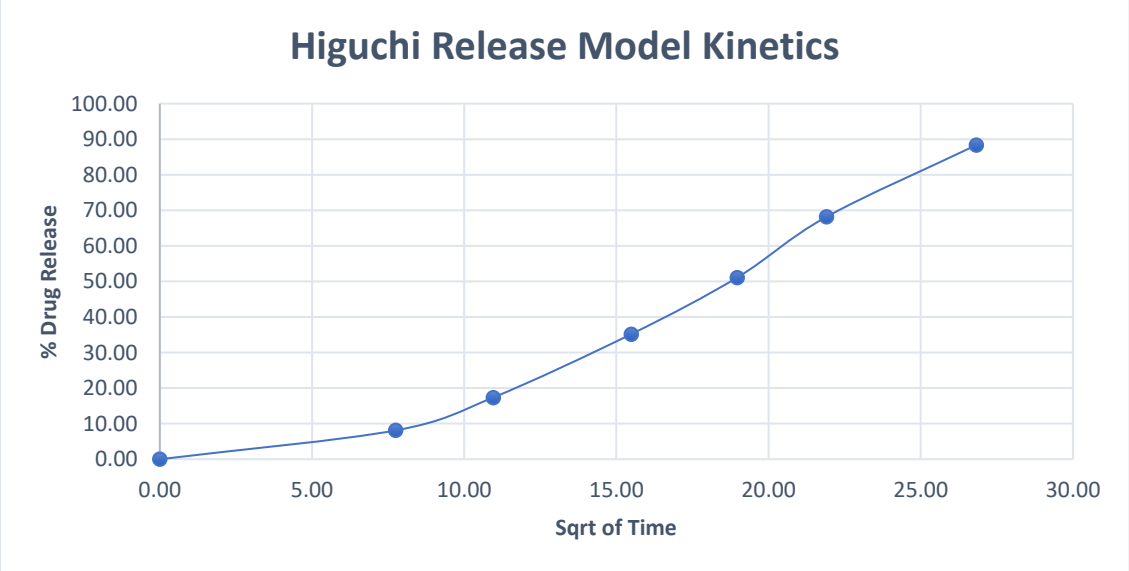

Figure 17: Higuchi Release kinetics for TNC

7.9 Stability study of Nanocapsules

Stability study was carried out for 3 months at at 40°C ± 2°C and 75% ± 5% relative humidity. The optimized batch TNC-6 was kept on stability to study the behavior of the formulation at elevated temperature so as to correlate how the formulation will behave at room temperature long term storage. The optimized formulation was evaluated before and after the stability interval for % Drug content, Particle size, zeta potential and SEM. The comparative results of stability study are given in Table 7.48

Table 22: Results of Stability study of TNC

	Parameters	At 0th day	After 90th days
1.	**Drug Content** (%)	95.23%	94.21%
2.	**Particle size**	101.1 nm	103.1 nm
3.	**Zeta Potential**	-21.6 mV	-21.3 mV
4.	**Phytochemical Analysis**	Alkaloids (-)	Alkaloids (-)
		Flavonoids (+)	Flavonoids (+)
		Terpenoids (+)	Terpenoids (+)
		Phenols (+)	Phenols (+)
		Tannins (+)	Tannins (+)
		Saponins (-)	Saponins (-)
		Glycosides (+)	Glycosides (+)
		Steroids (+)	Steroids (+)
5.	**SEM**	Size in nm	Size in nm

The formulation was found to be stable over the 90 days interval at at 40°C ± 2°C and 75% ± 5% relative humidity.